Editors' Suggestion

Observation of the $Y(4230)$ and a new structure in $e^+e^- \to K^+K^-J/\psi^*$

M. Ablikim(麦迪娜)[1]   M. N. Achasov[10,b]   P. Adlarson[68]   M. Albrecht[4]   R. Aliberti[28]   A. Amoroso[67A,67C]

M. R. An(安美儒)[32]   Q. An(安琪)[64,50]   X. H. Bai(白旭红)[58]   Y. Bai(白羽)[49]   O. Bakina[29]   R. Baldini Ferroli[23A]

I. Balossino[24A]   Y. Ban(班勇)[39,h]   V. Batozskaya[1,37]   D. Becker[28]   K. Begzsuren[26]   N. Berger[28]   M. Bertani[23A]

D. Bettoni[24A]   F. Bianchi[67A,67C]   J. Bloms[61]   A. Bortone[67A,67C]   I. Boyko[29]   R. A. Briere[5]   A. Brueggemann[61]

H. Cai(蔡浩)[69]   X. Cai(蔡啸)[1,50]   A. Calcaterra[23A]   G. F. Cao(曹国富)[1,55]   N. Cao(曹宁)[1,55]   S. A. Cetin[54A]

J. F. Chang(常劲帆)[1,50]   W. L. Chang(常万玲)[1,55]   G. Chelkov[29,a]   C. Chen(陈琛)[36]   G. Chen(陈刚)[1]

H. S. Chen(陈和生)[1,55]   M. L. Chen(陈玛丽)[1,50]   S. J. Chen(陈申见)[35]   T. Chen[1]   X. R. Chen(陈旭荣)[25,55]

X. T. Chen[1]   Y. B. Chen(陈元柏)[1,50]   Z. J. Chen(陈卓俊)[20,i]   W. S. Cheng(成伟帅)[67C]   X. Chu(初晓)[36]

G. Cibinetto[24A]   F. Cossio[67C]   J. J. Cui(崔佳佳)[42]   H. L. Dai(代洪亮)[1,50]   J. P. Dai(代建平)[71]   A. Dbeyssi[14]

R. E. de Boer[4]   D. Dedovich[29]   Z. Y. Deng(邓子艳)[1]   A. Denig[28]   I. Denysenko[29]   M. Destefanis[67A,67C]

F. De Mori[67A,67C]   Y. Ding(丁勇)[33]   J. Dong(董静)[1,50]   L. Y. Dong(董燎原)[1,55]   M. Y. Dong(董明义)[1,50,55]

X. Dong(董翔)[69]   S. X. Du(杜书先)[73]   P. Egorov[29,a]   Y. L. Fan(范玉兰)[69]   J. Fang(方建)[1,50]   S. S. Fang(房双世)[1,55]

W. X. Fang(方文兴)[1]   Y. Fang(方易)[1]   R. Farinelli[24A]   L. Fava[67B,67C]   F. Feldbauer[4]   G. Felici[23A]

C. Q. Feng(封常青)[64,50]   J. H. Feng(冯俊华)[51]   K Fischer[62]   M. Fritsch[4]   C. Fritzsch[61]   C. D. Fu(傅成栋)[1]

H. Gao(高涵)[55]   Y. N. Gao(高原宁)[39,h]   Yang Gao(高扬)[64,50]   S. Garbolino[67C]   I. Garzia[24A,24B]   P. T. Ge(葛潘婷)[69]

C. Geng(耿聪)[51]   E. M. Gersabeck[59]   A Gilman[62]   K. Goetzen[11]   L. Gong(龚丽)[33]   W. X. Gong(龚文煊)[1,50]

W. Gradl[28]   M. Greco[67A,67C]   M. H. Gu(顾旻皓)[1,50]   C. Y Guan(关春懿)[1,55]   A. Q. Guo(郭爱强)[25,55]

L. B. Guo(郭立波)[34]   R. P. Guo(郭如盼)[41]   Y. P. Guo(郭玉萍)[9,g]   A. Guskov[29,a]   T. T. Han(韩婷婷)[42]

W. Y. Han(韩文颖)[32]   X. Q. Hao(郝喜庆)[15]   F. A. Harris[57]   K. K. He(何凯凯)[47]   K. L. He(何康林)[1,55]

F. H. Heinsius[4]   C. H. Heinz[28]   Y. K. Heng(衡月昆)[1,50,55]   C. Herold[52]   M. Himmelreich[11,e]   T. Holtmann[4]

G. Y. Hou(侯国一)[1,55]   Y. R. Hou(侯颖锐)[55]   Z. L. Hou(侯治龙)[1]   H. M. Hu(胡海明)[1,55]   J. F. Hu[48,j]

T. Hu(胡涛)[1,50,55]   Y. Hu(胡誉)[1]   G. S. Huang(黄光顺)[64,50]   K. X. Huang(黄凯旋)[51]   L. Q. Huang(黄麟钦)[65]

L. Q. Huang(黄麟钦)[25,55]   X. T. Huang(黄性涛)[42]   Y. P. Huang(黄燕萍)[1]   Z. Huang[39,h]   T. Hussain[66]   N Hüsken[22,28]

W. Imoehl[22]   M. Irshad[64,50]   J. Jackson[22]   S. Jaeger[4]   S. Janchiv[26]   Q. Ji[1]   Q. P. Ji(姬清平)[15]

X. B. Ji(季晓斌)[1,55]   X. L. Ji(季筱璐)[1,50]   Y. Y. Ji(吉钰瑶)[42]   Z. K. Jia(贾泽坤)[64,50]   H. B. Jiang(姜侯兵)[42]

S. S. Jiang(姜赛赛)[32]   X. S. Jiang(江晓山)[1,50,55]   Y. Jiang[55]   J. B. Jiao(焦健斌)[42]   Z. Jiao(焦铮)[18]   S. Jin(金山)[35]

Y. Jin(金毅)[58]   M. Q. Jing(荆茂强)[1,55]   T. Johansson[68]   N. Kalantar-Nayestanaki[56]   X. S. Kang(康晓珅)[33]

R. Kappert[56]   M. Kavatsyuk[56]   B. C. Ke(柯百谦)[73]   I. K. Keshk[4]   A. Khoukaz[61]   P. Kiese[28]   R. Kiuchi[1]

R. Kliemt[11]   L. Koch[30]   O. B. Kolcu[54A]   B. Kopf[4]   M. Kuemmel[4]   M. Kuessner[4]   A. Kupsc[37,68]   W. Kühn[30]

J. J. Lane[59]   J. S. Lange[30]   P. Larin[14]   A. Lavania[21]   L. Lavezzi[67A,67C]   Z. H. Lei(雷祚弘)[64,50]   H. Leithoff[28]

M. Lellmann[28]   T. Lenz[28]   C. Li(李聪)[36]   C. Li(李翠)[40]   C. H. Li(李春花)[32]   Cheng Li(李澄)[64,50]

D. M. Li(李德民)[73]   F. Li(李飞)[1,50]   G. Li(李刚)[1]   H. Li(李贺)[44]   H. Li[64,50]   H. B. Li(李海波)[1,55]

H. J. Li(李惠静)[15]   H. N. Li[48,j]   J. Q. Li[4]   J. S. Li(李静舒)[51]   J. W. Li(李井文)[42]   Ke Li(李科)[1]   L. J Li[1]

L. K. Li(李龙科)[1]   Lei Li(李蕾)[3]   M. H. Li(李明浩)[36]   P. R. Li(李培荣)[31,k,l]   S. X. Li(李素娴)[9]   S. Y. Li(栗帅迎)[53]

T. Li(李腾)[42]   W. D. Li(李卫东)[1,55]   W. G. Li(李卫国)[1]   X. H. Li(李旭红)[64,50]   X. L. Li(李晓玲)[42]

Xiaoyu Li(李晓宇)[1,55]   Z. Y. Li(李紫源)[51]   H. Liang(梁浩)[1,55]   H. Liang(梁昊)[64,50]   H. Liang(梁浩)[27]

Y. F. Liang(梁勇飞)[46]   Y. T. Liang(梁羽铁)[25,55]   G. R. Liao(廖广睿)[12]   L. Z. Liao(廖龙洲)[42]   J. Libby[21]

A. Limphirat[52]   C. X. Lin[51]   D. X. Lin(林德旭)[25,55]   T. Lin[1]   B. J. Liu(刘北江)[1]   C. X. Liu(刘春秀)[1]   D. Liu[14,64]

F. H. Liu(刘福虎)[45]   Fang Liu(刘芳)[1]   Feng Liu(刘峰)[6]   G. M. Liu[48,j]   H. Liu[31,k,l]   H. M. Liu(刘怀民)[1,55]

Huanhuan Liu(刘欢欢)[1]   Huihui Liu(刘汇慧)[16]   J. B. Liu(刘建北)[64,50]   J. L. Liu(刘佳俊)[65]   J. Y. Liu(刘晶译)[1,55]

K. Liu(刘凯)[1]   K. Y. Liu(刘魁勇)[33]   Ke Liu(刘珂)[17]   L. Liu(刘亮)[64,50]   M. H. Liu(刘美宏)[9,g]   P. L. Liu(刘佩莲)[1]

Q. Liu(刘倩)[55]   S. B. Liu(刘树彬)[64,50]   T. Liu(刘桐)[9,g]   W. K. Liu(刘维克)[36]   W. M. Liu(刘卫民)[64,50]

X. Liu(刘翔)[31,k,l]   Y. Liu(刘英)[31,k,l]   Y. B. Liu(刘玉斌)[36]   Z. A. Liu(刘振安)[1,50,55]   Z. Q. Liu(刘智青)[42]

X. C. Lou(娄辛丑)[1,50,55]   F. X. Lu(卢飞翔)[51]   H. J. Lu(吕海江)[18]   J. G. Lu(吕军光)[1,50]   X. L. Lu(陆小玲)[1]

Y. Lu(卢宇)[1]   Y. P. Lu(卢云鹏)[1,50]   Z. H. Lu(卢泽辉)[1]   C. L. Luo(罗成林)[34]   M. X. Luo(罗民兴)[72]   T. Luo(罗涛)[9,g]

X. L. Luo(罗小兰)[1,50]   X. R. Lyu(吕晓睿)[55]   Y. F. Lyu(吕翌丰)[36]   F. C. Ma(马凤才)[33]   H. L. Ma(马海龙)[1]

L. L. Ma(马连良)[42]   M. M. Ma(马明明)[1,55]   Q. M. Ma(马秋梅)[1]   R. Q. Ma(马润秋)[1,55]   R. T. Ma(马瑞廷)[55]

X. Y. Ma(马骁妍)[1,50]   Y. Ma(马尧)[39,h]   F. E. Maas[14]   M. Maggiora[67A,67C]   S. Maldaner[4]   S. Malde[62]   Q. A. Malik[66]

A. Mangoni[23B]   Y. J. Mao(冒亚军)[39,h]   Z. P. Mao(毛泽普)[1]   S. Marcello[67A,67C]   Z. X. Meng(孟召霞)[58]

J. G. Messchendorp[56,d]   G. Mezzadri[24A]   H. Miao[1]   T. J. Min(闵天觉)[35]   R. E. Mitchell[22]   X. H. Mo(莫晓虎)[1,50,55]

N. Yu. Muchnoi[10,b]   H. Muramatsu[60]   Y. Nefedov[29]   F. Nerling[11,e]   I. B. Nikolaev[10,b]   Z. Ning(宁哲)[1,50]   S. Nisar[8,m]

Y. Niu(牛艳)[42]   S. L. Olsen[55]   Q. Ouyang(欧阳群)[1,50,55]   S. Pacetti[23B,23C]   X. Pan(潘祥)[9,g]   Y. Pan[59]   A. Pathak[1]

A. Pathak[27]   M. Pelizaeus[4]   H. P. Peng(彭海平)[64,50]   K. Peters[11,e]   J. Pettersson[68]   J. L. Ping(平加伦)[34]

R. G. Ping(平荣刚)[1,55]   S. Plura[28]   S. Pogodin[29]   R. Poling[60]   V. Prasad[64,50]   F. Z. Qi(齐法制)[1]   H. Qi(齐航)[64,50]

H. R. Qi(漆红荣)[53]   M. Qi(祈鸣)[35]   T. Y. Qi(齐天钰)[9,g]   S. Qian(钱森)[1,50]   W. B. Qian(钱文斌)[55]   Z. Qian(钱圳)[51]

C. F. Qiao(乔从丰)[55]   J. J. Qin(秦佳佳)[65]   L. Q. Qin(秦丽清)[12]   X. P. Qin(覃潇平)[9,g]   X. S. Qin(秦小帅)[42]

Z. H. Qin(秦中华)[1,50]   J. F. Qiu(邱进发)[1]   S. Q. Qu(屈三强)[53]   S. Q. Qu[36]   K. H. Rashid[66]   C. F. Redmer[28]

K. J. Ren(任旷洁)[32]   A. Rivetti[67C]   V. Rodin[56]   M. Rolo[67C]   G. Rong(荣刚)[1,55]   Ch. Rosner[14]   S. N. Ruan(阮氏宁)[36]

H. S. Sang[64]   A. Sarantsev[29,c]   Y. Schelhaas[28]   C. Schnier[4]   K. Schoenning[68]   M. Scodeggio[24A,24B]

K. Y. Shan(尚科羽)[9,g]   W. Shan(单葳)[19]   X. Y. Shan(单心钰)[64,50]   J. F. Shangguan(上官剑锋)[47]

L. G. Shao(邵立港)[1,55]   M. Shao(邵明)[64,50]   C. P. Shen(沈成平)[9,g]   H. F. Shen(沈宏飞)[1,55]   X. Y. Shen(沈肖雁)[1,55]

B.-A. Shi(施伯安)[55]   H. C. Shi(石煌超)[64,50]   J. Y. Shi(石京燕)[1]   R. S. Shi(师荣盛)[1,55]   X. Shi(史欣)[1,50]

X. D Shi(师晓东)[64,50]   J. J. Song(宋娇娇)[15]   W. M. Song(宋维民)[27,1]   Y. X. Song(宋昀轩)[39,h]   S. Sosio[67A,67C]

S. Spataro[67A,67C]   F. Stieler[28]   K. X. Su(苏可馨)[69]   P. P. Su(苏彭彭)[47]   Y.-J. Su(粟杨捷)[55]   G. X. Sun(孙功星)[1]

H. Sun[55]   H. K. Sun(孙浩凯)[1]   J. F. Sun(孙俊峰)[15]   L. Sun(孙亮)[69]   S. S. Sun(孙胜森)[1,55]   T. Sun(孙童)[1,55]

W. Y. Sun(孙文玉)[27]   X Sun(孙翔)[20,i]   Y. J. Sun(孙勇杰)[64,50]   Y. Z. Sun(孙永昭)[1]   Z. T. Sun(孙振田)[42]

Y. H. Tan(谭英华)[69]   Y. X. Tan(谭雅星)[64,50]   C. J. Tang(唐昌建)[46]   G. Y. Tang(唐光毅)[1]   J. Tang(唐健)[51]

L. Y Tao(陶璐燕)[65]   Q. T. Tao(陶秋田)[20,i]   J. X. Teng(滕佳秀)[64,50]   V. Thoren[68]   W. H. Tian(田文辉)[44]

Y. Tian(田野)[25,55]   I. Uman[54B]   B. Wang(王斌)[1]   B. L. Wang(王滨龙)[55]   D. Y. Wang(王大勇)[39,h]   F. Wang(王菲)[65]

H. J. Wang(王泓鉴)[31,k,l]   H. P. Wang(王宏鹏)[1,55]   K. Wang(王科)[1,50]   L. L. Wang(王亮亮)[1]   M. Wang(王萌)[42]

M. Z. Wang[39,h]   Meng Wang(王蒙)[1,55]   S. Wang(王顺)[9,g]   T. Wang(王婷)[9,g]   T. J. Wang(王腾蛟)[36]

W. Wang(王为)[51]   W. H. Wang(王文欢)[69]   W. P. Wang(王维平)[64,50]   X. Wang(王轩)[39,h]   X. F. Wang(王雄飞)[31,k,l]

X. L. Wang(王小龙)[9,g]   Y. D. Wang(王雅迪)[38]   Y. F. Wang(王贻芳)[1,50,55]   Y. H. Wang(王英豪)[40]

Y. Q. Wang(王雨晴)[1]   Ying Wang[51]   Z. Wang(王铮)[1,50]   Z. Y. Wang(王至勇)[1,55]   Ziyi Wang(王子一)[55]

D. H. Wei(魏代会)[12]   F. Weidner[61]   S. P. Wen(文硕频)[1]   D. J. White[59]   U. Wiedner[4]   G. Wilkinson[62]   M. Wolke[68]

L. Wollenberg[4]   J. F. Wu(吴金飞)[1,55]   L. H. Wu(伍灵慧)[1]   L. J. Wu(吴连近)[1,55]   X. Wu(吴潇)[9,g]

X. H. Wu(伍雄浩)[27]   Y. Wu[64]   Z. Wu(吴智)[1,50]   L. Xia(夏磊)[64,50]   T. Xiang(相腾)[39,h]   D. Xiao(肖栋)[31,k,l]

H. Xiao(肖浩)[9,g]   S. Y. Xiao(肖素玉)[1]   Y. L. Xiao(肖云龙)[9,g]   Z. J. Xiao(肖振军)[34]   X. H. Xie(谢昕海)[39,h]

Y. Xie(谢勇)[42]   Y. G. Xie(谢宇广)[1,50]   Y. H. Xie(谢跃红)[6]   Z. P. Xie(谢智鹏)[64,50]   T. Y. Xing(邢天宇)[1,55]

C. F. Xu[1]   C. J. Xu(许创杰)[51]   G. F. Xu(许国发)[1]   Q. J. Xu(徐庆君)[13]   S. Y. Xu[63]   X. P. Xu(徐新平)[47]

Y. C. Xu(胥英超)[55]   F. Yan(严芳)[9,g]   L. Yan(严亮)[9,g]   W. B. Yan(鄢文标)[64,50]   W. C. Yan(闫文成)[73]

H. J. Yang(杨海军)[43,f]   H. L. Yang(杨昊霖)[27]   H. X. Yang(杨洪勋)[1]   L. Yang(杨玲)[44]   S. L. Yang[55]

Tao Yang(杨涛)[1]   Y. X. Yang(杨逸翔)[1,55]   Yifan Yang(杨翊凡)[1,55]   M. Ye(叶梅)[1,50]   M. H. Ye(叶铭汉)[7]

J. H. Yin(殷俊昊)[1]   Z. Y. You(尤郑昀)[51]   B. X. Yu(俞伯祥)[1,50,55]   C. X. Yu(喻纯旭)[36]   G. Yu(余刚)[1,55]

T. Yu(于涛)[65]   C. Z. Yuan(苑长征)[1,55]   L. Yuan(袁丽)[2]   S. C. Yuan[1]   X. Q. Yuan(袁晓庆)[1]   Y. Yuan(袁野)[1,55]

Z. Y. Yuan(袁朝阳)[51]   C. X. Yue(岳崇兴)[32]   A. A. Zafar[66]   F. R. Zeng(曾凡蕊)[42]   X. Zeng(曾鑫)[6]

Y. Zeng(曾云)[20,i]   Y. H. Zhan(詹永华)[51]   A. Q. Zhang(张安庆)[1]   B. L. Zhang[1]   B. X. Zhang(张丙新)[1]

D. H. Zhang(张丹昊)[36]   G. Y. Zhang(张广义)[15]   H. Zhang[64]   H. H. Zhang(张宏浩)[51]   H. H. Zhang(张宏宏)[27]

H. Y. Zhang(章红宇)[1,50]   J. L. Zhang(张杰磊)[70]   J. Q. Zhang(张敬庆)[34]   J. W. Zhang(张家文)[1,50,55]   J. X. Zhang[31,k,l]

J. Y. Zhang(张建勇)[1]   J. Z. Zhang(张景芝)[1,55]   Jianyu Zhang(张剑宇)[1,55]   Jiawei Zhang(张嘉伟)[1,55]

L. M. Zhang(张黎明)[53]   L. Q. Zhang(张丽青)[51]   Lei Zhang(张雷)[35]   P. Zhang[1]   Q. Y. Zhang(张秋岩)[32,73]

Shulei Zhang(张书磊)[20,i]   X. D. Zhang(张小东)[38]   X. M. Zhang[1]   X. Y. Zhang(张旭颜)[42]   X. Y. Zhang(张学尧)[47]

Y. Zhang[62]   Y. T. Zhang(张亚腾)[73]   Y. H. Zhang(张银鸿)[1,50]   Yan Zhang(张言)[64,50]   Yao Zhang(张瑶)[1]

Z. H. Zhang[1]   Z. Y. Zhang(张振宇)[36]   Z. Y. Zhang(张子羽)[69]   G. Zhao(赵光)[1]   J. Zhao(赵静)[32]

J. Y. Zhao(赵静宜)[1,55]   J. Z. Zhao(赵京周)[1,50]   Lei Zhao(赵雷)[64,50]   Ling Zhao(赵玲)[1]   M. G. Zhao(赵明刚)[36]

Q. Zhao(赵强)[1]   S. J. Zhao(赵书俊)[73]   Y. B. Zhao(赵豫斌)[1,50]   Y. X. Zhao(赵宇翔)[25,55]   Z. G. Zhao(赵政国)[64,50]

A. Zhemchugov[29,a]   B. Zheng(郑波)[65]   J. P. Zheng(郑建平)[1,50]   Y. H. Zheng(郑阳恒)[55]   B. Zhong(钟彬)[34]

C. Zhong(钟翠)[65]   X. Zhong(钟鑫)[51]   H. Zhou(周航)[42]   L. P. Zhou(周利鹏)[1,55]   X. Zhou(周详)[69]

X. K. Zhou(周晓康)[55]   X. R. Zhou(周小蓉)[64,50]   X. Y. Zhou(周兴玉)[32]   Y. Z. Zhou(周祎卓)[9,g]   J. Zhu(朱江)[36]

K. Zhu[1]   K. J. Zhu(朱科军)[1,50,55]   L. X. Zhu(朱琳萱)[55]   S. H. Zhu(朱世海)[63]   T. J. Zhu[70]   W. J. Zhu(朱文静)[9,g]

Y. C. Zhu(朱莹春)[64,50]   Z. A. Zhu(朱自安)[1,55]   B. S. Zou(邹冰松)[1]   J. H. Zou(邹佳恒)[1]

(BESIII Collaboration)

[1]Institute of High Energy Physics, Beijing 100049, China
[2]Beihang University, Beijing 100191, China
[3]Beijing Institute of Petrochemical Technology, Beijing 102617, China
[4]Bochum Ruhr-University, D-44780 Bochum, Germany
[5]Carnegie Mellon University, Pittsburgh, Pennsylvania 15213, USA
[6]Central China Normal University, Wuhan 430079, China
[7]China Center of Advanced Science and Technology, Beijing 100190, China
[8]COMSATS University Islamabad, Lahore Campus, Defence Road, Off Raiwind Road, 54000 Lahore, Pakistan
[9]Fudan University, Shanghai 200433, China
[10]G.I. Budker Institute of Nuclear Physics SB RAS (BINP), Novosibirsk 630090, Russia
[11]GSI Helmholtzcentre for Heavy Ion Research GmbH, D-64291 Darmstadt, Germany
[12]Guangxi Normal University, Guilin 541004, China
[13]Hangzhou Normal University, Hangzhou 310036, China
[14]Helmholtz Institute Mainz, Staudinger Weg 18, D-55099 Mainz, Germany
[15]Henan Normal University, Xinxiang 453007, China
[16]Henan University of Science and Technology, Luoyang 471003, China
[17]Henan University of Technology, Zhengzhou 450001, China
[18]Huangshan College, Huangshan 245000, China
[19]Hunan Normal University, Changsha 410081, China
[20]Hunan University, Changsha 410082, China
[21]Indian Institute of Technology Madras, Chennai 600036, India
[22]Indiana University, Bloomington, Indiana 47405, USA
[23A]INFN Laboratori Nazionali di Frascati, INFN Laboratori Nazionali di Frascati, I-00044, Frascati, Italy
[23B]INFN Laboratori Nazionali di Frascati, INFN Sezione di Perugia, I-06100, Perugia, Italy
[23C]INFN Laboratori Nazionali di Frascati, University of Perugia, I-06100, Perugia, Italy
[24A]INFN Sezione di Ferrara, INFN Sezione di Ferrara, I-44122, Ferrara, Italy
[24B]INFN Sezione di Ferrara, University of Ferrara, I-44122, Ferrara, Italy
[25]Institute of Modern Physics, Lanzhou 730000, China
[26]Institute of Physics and Technology, Peace Ave. 54B, Ulaanbaatar 13330, Mongolia
[27]Jilin University, Changchun 130012, China

[28]Johannes Gutenberg University of Mainz, Johann-Joachim-Becher-Weg 45, D-55099 Mainz, Germany

[29]Joint Institute for Nuclear Research, 141980 Dubna, Moscow region, Russia

[30]Justus-Liebig-Universitaet Giessen, II. Physikalisches Institut, Heinrich-Buff-Ring 16, D-35392 Giessen, Germany

[31]Lanzhou University, Lanzhou 730000, China

[32]Liaoning Normal University, Dalian 116029, China

[33]Liaoning University, Shenyang 110036, China

[34]Nanjing Normal University, Nanjing 210023, China

[35]Nanjing University, Nanjing 210093, China

[36]Nankai University, Tianjin 300071, China

[37]National Centre for Nuclear Research, Warsaw 02-093, Poland

[38]North China Electric Power University, Beijing 102206, China

[39]Peking University, Beijing 100871, China

[40]Qufu Normal University, Qufu 273165, China

[41]Shandong Normal University, Jinan 250014, China

[42]Shandong University, Jinan 250100, China

[43]Shanghai Jiao Tong University, Shanghai 200240, China

[44]Shanxi Normal University, Linfen 041004, China

[45]Shanxi University, Taiyuan 030006, China

[46]Sichuan University, Chengdu 610064, China

[47]Soochow University, Suzhou 215006, China

[48]South China Normal University, Guangzhou 510006, China

[49]Southeast University, Nanjing 211100, China

[50]State Key Laboratory of Particle Detection and Electronics, Beijing 100049, Hefei 230026, China

[51]Sun Yat-Sen University, Guangzhou 510275, China

[52]Suranaree University of Technology, University Avenue 111, Nakhon Ratchasima 30000, Thailand

[53]Tsinghua University, Beijing 100084, China

[54A]Turkish Accelerator Center Particle Factory Group, Istinye University, 34010, Istanbul, Turkey

[54B]Turkish Accelerator Center Particle Factory Group, Near East University, Nicosia, North Cyprus, Mersin 10, Turkey

[55]University of Chinese Academy of Sciences, Beijing 100049, China

[56]University of Groningen, NL-9747 AA Groningen, The Netherlands

[57]University of Hawaii, Honolulu, Hawaii 96822, USA

[58]University of Jinan, Jinan 250022, China

[59]University of Manchester, Oxford Road, Manchester, M13 9PL, United Kingdom

[60]University of Minnesota, Minneapolis, Minnesota 55455, USA

[61]University of Muenster, Wilhelm-Klemm-Str. 9, 48149 Muenster, Germany

[62]University of Oxford, Keble Rd, Oxford, UK OX13RH

[63]University of Science and Technology Liaoning, Anshan 114051, China

[64]University of Science and Technology of China, Hefei 230026, China

[65]University of South China, Hengyang 421001, China

[66]University of the Punjab, Lahore-54590, Pakistan

[67A]University of Turin and INFN, University of Turin, I-10125, Turin, Italy

[67B]University of Turin and INFN, University of Eastern Piedmont, I-15121, Alessandria, Italy

[67C]University of Turin and INFN, INFN, I-10125, Turin, Italy

[68]Uppsala University, Box 516, SE-75120 Uppsala, Sweden

[69]Wuhan University, Wuhan 430072, China

[70]Xinyang Normal University, Xinyang 464000, China

[71]Yunnan University, Kunming 650500, China

[72]Zhejiang University, Hangzhou 310027, China

[73]Zhengzhou University, Zhengzhou 450001, China

[a]Also at the Moscow Institute of Physics and Technology, Moscow 141700, Russia

[b]Also at the Novosibirsk State University, Novosibirsk, 630090, Russia

[c]Also at the NRC "Kurchatov Institute", PNPI, 188300, Gatchina, Russia

[d]Currently at Istanbul Arel University, 34295 Istanbul, Turkey

[e]Also at Goethe University Frankfurt, 60323 Frankfurt am Main, Germany

[f]Also at Key Laboratory for Particle Physics, Astrophysics and Cosmology, Ministry of Education; Shanghai Key Laboratory for Particle Physics and Cosmology; Institute of Nuclear and Particle Physics, Shanghai 200240, China

[g]Also at Key Laboratory of Nuclear Physics and Ion-beam Application (MOE) and Institute of Modern Physics, Fudan University, Shanghai 200443, China

[h]Also at State Key Laboratory of Nuclear Physics and Technology, Peking University, Beijing 100871, China

[i]Also at School of Physics and Electronics, Hunan University, Changsha 410082, China

[j]Also at Guangdong Provincial Key Laboratory of Nuclear Science, Institute of Quantum Matter, South China Normal University, Guangzhou 510006, China

[k]Also at Frontiers Science Center for Rare Isotopes, Lanzhou University, Lanzhou 730000, China

[l]Also at Lanzhou Center for Theoretical Physics, Lanzhou University, Lanzhou 730000, China

[m]Also at the Department of Mathematical Sciences, IBA, Karachi, Pakistan

Abstract: The cross sections of $e^+e^- \to K^+K^-J/\psi$ at center-of-mass energies from 4.127 to 4.600 GeV are measured based on 15.6 fb^{-1} data collected with the BESIII detector operating at the BEPCII storage ring. Two resonant

structures are observed in the line shape of the cross sections. The mass and width of the first structure are measured to be $(4225.3 \pm 2.3 \pm 21.5)$ MeV and $(72.9 \pm 6.1 \pm 30.8)$ MeV, respectively. They are consistent with those of the established $Y(4230)$. The second structure is observed for the first time with a statistical significance greater than 8σ, denoted as $Y(4500)$. Its mass and width are determined to be $(4484.7 \pm 13.3 \pm 24.1)$ MeV and $(111.1 \pm 30.1 \pm 15.2)$ MeV, respectively. The first presented uncertainties are statistical and the second ones are systematic. The product of the electronic partial width with the decay branching fraction $\Gamma(Y(4230) \to e^+e^-)\mathcal{B}(Y(4230) \to K^+K^-J/\psi)$ is reported.

I. INTRODUCTION

Recent discoveries of charmonium-like states expand our perspective of the hadron spectrum around the τ-charm energy region, and provide excellent laboratories to study perturbative and non-perturbative strong interaction. The dynamic, however, is more complex than the one of conventional mesons due to possible additional degrees of freedom. Therefore, their nature has not yet been established despite many different speculations about them being hybrids, tetra-quarks, molecules, cusp effects, and so on [1].

Among the exotic states, the $Y(4230)$ state, previously called $Y(4260)$, is the first observed vector charmonium-like state. It was discovered in $e^+e^- \to \pi^+\pi^- J/\psi$ channel by the BaBar Collaboration using initial-state-radiation (ISR) technique [2], and confirmed by CLEO [3] and Belle [4]. In addition, the $Y(4230)$ state was observed in various modes by BESIII, including $e^+e^- \to \pi\pi J/\psi$ [5–7], $\pi^+\pi^- h_c$ [8], $\pi\pi\psi(2S)$ [9–11], $\omega\chi_{c0}$ [12, 13], and $\pi^+ D^0 D^{*-} + c.c.$ [14]. It was also found to decay into $X(3872)$ via radiative transition [15] and to $Z_c(3900)$ via pion transition [6]. A better understanding of its internal structure and quark components is crucial, and it will also be helpful to understand the series of the tetra-quark candidates [16].

Two recent measurements on the cross sections of $e^+e^- \to \eta J/\psi$ [17] and $e^+e^- \to \eta' J/\psi$ [18] indicate a considerable strange quark component in $Y(4230)$. This hypothesis was analyzed in Ref. [19]. However, a concrete conclusion is still missing due to the large uncertainty. Thus a measurement of $Y(4230) \to K\bar{K}J/\psi$ is important to clarify the puzzle by comparison with the results of $Y(4230) \to \pi\pi J/\psi$. The first evidence for $Y(4230) \to K^+K^-J/\psi$ was found by CLEO [20]. Later, the cross sections of $e^+e^- \to K^+K^-J/\psi$ at center-of-mass (c.m.) energies between threshold and 6.0 GeV were measured for the first time via ISR process [21] and was updated [22] by Belle. No significant signal was observed in both measurements, and an upper limit $\mathcal{B}(Y(4230) \to K^+K^-J/\psi)\Gamma(Y(4230) \to e^+e^-) < 1.7$ eV at 90% confidence level was obtained. Here and following the natural unit system is adopted, i.e., $\hbar = c = 1$. Recently, BESIII

has measured the cross sections of $e^+e^- \to K\bar{K}J/\psi$ at c.m. energies from 4.189 to 4.600 GeV with an integrated luminosity ($\mathcal{L}_{int}$) of 4.7 fb^{-1} [23], and no significant signal of the $Y(4230)$ is observed too. In Refs. [21–23], a structure around $\sqrt{s} = 4.5$ GeV was seen, though the statistics is too small to identify its properties. The structure with higher mass is consistent with the calculation by Ref. [24], which suggests a conventional charmonium state $\psi(4500)$ with mass of $4489 - 4529$ MeV by the 5S-4D mixing scheme. It is also consistent with a virtual state predicted in Ref. [25], where the mass of the heavy-anti-heavy hadronic molecule is calculated to be $4483 - 4503$ MeV that is just below the $D_s \bar{D}_{s1}$ threshold. Meanwhile, Ref. [26] predicts an exotic state with $c\bar{c}s\bar{s}$ component in quenched lattice quantum chromodynamics with exact chiral symmetry, and its mass is predicted to be (4450 ± 100) MeV.

In this Letter, we present an updated measurement of the Born cross sections of $e^+e^- \to K^+K^-J/\psi$ at the c.m. energies from 4.127 to 4.600 GeV, using data samples composed of twenty-eight c.m. energy points [27, 28] with $\mathcal{L}_{int} = 15.6$ fb^{-1} [29, 30], collected at the BESIII detector operating at the BEPCII storage ring [31]. These samples are about three times in luminosity compared with that used in Ref. [23], and they overlap at eleven energy points. The added points are mainly around the $Y(4230)$ mass region, except two points around 4.5 GeV that are crucial for determining the line shape of $Y(4500)$. Furthermore, although previously in Ref. [23] a full reconstruction method is applied, considering the low efficiency of kaon reconstruction with low momentum, a new partial reconstruction method is applied improving significantly the efficiency.

II. DATA ANALYSIS

The BESIII detector is described in detail in Refs. [31, 32]. The geant4-based [33] Monte Carlo (MC) simulation software framework boost [34], which consists of detector geometry and its response, is used to produce large simulated event samples. These samples are used to optimize the event selection criteria, determine the detection efficiency, evaluate the ISR correction factor, and es-

timate background contributions. The signal events are generated at each c.m. energy, where signal events include $e^+e^- \to K^+K^-J/\psi$ (phase space (PHSP) model), $f_0(980)J/\psi$, and $f_2(1270)J/\psi$. Both $f_0(980)$ and $f_2(1270)$ decay into K^+K^-, and J/ψ decays into one lepton pair ($\mu^+\mu^-/e^+e^-$). The simulation includes the beam energy spread and ISR in the e^+e^- annihilation modelled with the generator kkmc [35, 36] and evtgen [37, 38], where the angular distributions according to spin and parity are considered by the specific models implemented in the generator. The final state radiation effect associated with leptons is handled by the photos package [39]. The potential backgrounds are estimated by the inclusive MC sample, that includes the production of open charm processes, the ISR production of vector charmonium(-like) states, and the continuum processes incorporated in kkmc. All particle decays are modelled with evtgen using branching fractions either taken from the Particle Data Group [40], when available, or otherwise estimated with lundcharm [41, 42].

A pair of leptons ($e^+e^-/\mu^+\mu^-$) and at least one kaon is required for a signal candidate. For each track, the polar angle θ, with respect to the symmetry axis of the multiple drift chamber, must satisfy $|\cos\theta| < 0.93$, and the point of the closest approach to the e^+e^- interaction point must be less than 10.0 cm in the beam direction and 1.0 cm in the plane perpendicular to the beam direction. Each charged track with momentum larger than 1.0 GeV in the laboratory frame is assumed to be a lepton. The ratio of the energy deposited in the electromagnetic calorimeter over the momentum of each lepton candidate is required to be greater than 0.8 for electrons and less than 0.8 for muons. For particle identification (PID), the energy loss in the main drift chamber and the time measured with the time-of-flight system are combined to calculate the confidence levels (*C.L.*) with kaon and pion hypotheses, and the confidence level is required to satisfy $C.L.(K) > 0.001$ and $C.L.(K) > C.L.(\pi)$ for each kaon candidate. In order to improve resolution and suppress backgrounds, a vertex fit and a kinematic fit with one constraint on the mass of the missing kaon are performed. If there is more than one kaon track candidate, the selected one has the smallest χ^2_F, defined as the sum of the χ^2 of vertex and kinematic fits and required to be less than 20. To remove radiative Bhabha background, where the radiative photon would convert into an e^+e^- pair, all pairs of oppositely charged tracks must have an opening angle $\cos(\theta_{open}) < 0.98$ for the e^+e^- mode. For the $\mu^+\mu^-$ mode, the penetration depth for one of the muon candidate in the muon counter is required to be greater than 40 cm to remove hadron backgrounds.

After applying the aforementioned event selection, the invariant mass distributions of e^+e^- and $\mu^+\mu^-$ are shown in Fig. 1 with all data samples. The signal region of J/ψ is defined as a region with 2.5 times of the mass
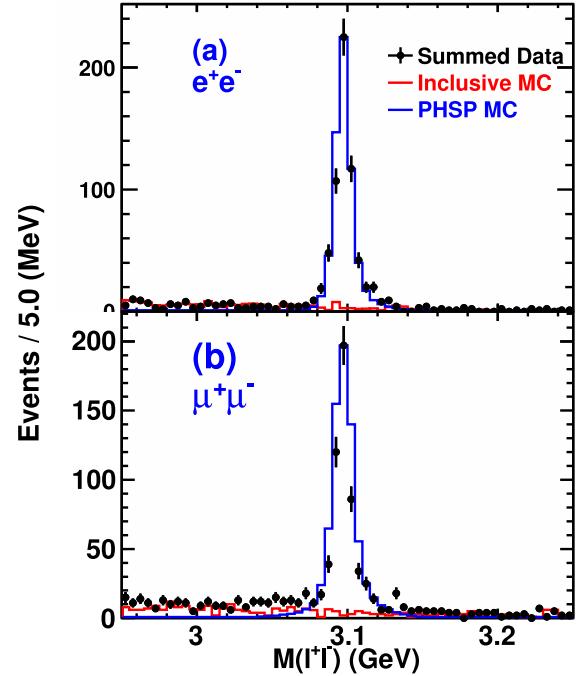
Fig. 1. (color online) The invariant mass distributions of the lepton pairs from different J/ψ decay modes. (a) is e^+e^- mode, (b) is $\mu^+\mu^-$ mode, where the dots with error bar indicate data, the blue line histograms indicate PHSP signal MC sample, the red line histograms indicate backgrounds from inclusive MC sample.

resolution, and the side band regions are taken as the same size as the signal with 0.01 GeV gap from the signal region. The distributions of $M(\ell^+\ell^-)$ at all the energies are presented in Appendix 1, where $\ell^+\ell^-$ is either e^+e^- or $\mu^+\mu^-$. There are no peaking backgrounds based on the study of inclusive MC samples. The yields of signals (N^{obs}) are obtained from background subtraction and the corresponding uncertainties are estimated by the profile likelihood method [43].

To explore potential intermediate states, the invariant mass distributions of K^+K^- and K^+J/ψ are shown in Fig. 2, with all data samples, PHSP signal MC samples, and the weighted signal MC samples, where PHSP and weighted signal MC samples are both normalized to data. There is no obvious structure in the KJ/ψ invariant mass distributions. The distributions of invariant mass of K^+K^- show signs of mesons $f_0(980)$ and $f_2(1270)$. These distributions roughly match with the theoretical calculation at $\sqrt{s} = 4.23$ and 4.26 GeV [44], while the corresponding predictions are still missing at higher energy regions. We extract the contributions of different components (PHSP, $f_0(980)$, $f_2(1270)$) by fitting to the data samples with large signal yields ($N^{obs} > 55$), then expanding the results to the smaller samples by linear interpolation. The efficiency of event selection (ε) is calculated by the sum of weighted efficiencies of these components.
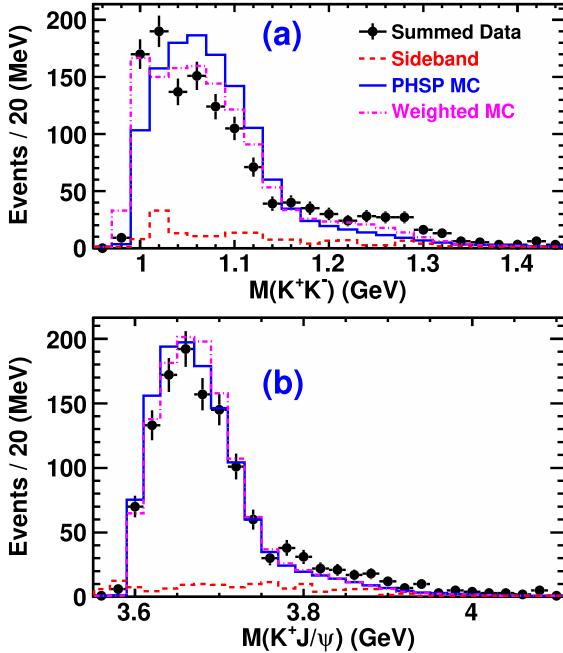
Fig. 2. (color online) (a) and (b) are distributions of $M(K^+K^-)$ and $M(K^+J/\psi)$, respectively. The black dots with error bars indicate data from the J/ψ signal region with all data samples, the red dashed curves indicate data from J/ψ side band regions, the blue solid curves indicate PHSP signal MC sample, and the yank dashed-dot curves indicated the weighted signal MC sample.

III. BORN CROSS SECTION AND RESONANT PARAMETER

The Born cross section of $e^+e^- \rightarrow K^+K^-J/\psi$ at each energy is obtained by

$$\sigma^B(\sqrt{s}) = \frac{N^{\text{obs}}}{\mathcal{L}_{\text{int}} \cdot \varepsilon \cdot (1+\delta)_{\text{ISR}} \cdot \frac{1}{|1-\Pi|^2} \cdot \mathcal{B}(J/\psi \rightarrow \ell^+\ell^-)}, \quad (1)$$

where $\frac{1}{|1-\Pi|^2}$ is the vacuum polarization factor calculated by QED [45], $\mathcal{B}(J/\psi \rightarrow \ell^+\ell^-)$ is the branching fraction that is quoted as $(11.93 \pm 0.05)\%$ [40], $(1+\delta)_{\text{ISR}}$ is the radiative correction factor obtained by an iteration method, described in details in Ref. [46]. The results of Born cross sections are listed in Appendix 2. Compared with the previous BESIII measurements [23], the Born cross sections at the same c.m. energies are consistent, and the precision is slightly improved. The observation of two clear structures in the distribution of the cross sections is due to more data samples used.

A maximum likelihood fit is applied to the dressed cross sections ($\sigma^D(\sqrt{s})$, including vacuum polarization effects) of $e^+e^- \rightarrow K^+K^-J/\psi$ to determine the parameters

of the resonant structures, and the dressed cross sections are shown in Fig. 3. The likelihood is constructed taking the fluctuations of the number of signal events into account. Its definition is described in Appendix 3. The fit function is parameterized as a coherent sum of two relativistic Breit-Wigner (BW) functions

$$\sigma^D(\sqrt{s}) = |\text{BW}_1(\sqrt{s}) \cdot e^{i\varphi} + \text{BW}_2(\sqrt{s})|^2, \quad (2)$$

where φ is the relative phase angle, and

$$\text{BW}(\sqrt{s}) = \frac{M}{\sqrt{s}} \cdot \frac{\sqrt{12\pi\Gamma_{ee}\Gamma_{\text{tot}}\mathcal{B}}}{s - M^2 + iM\Gamma_{\text{tot}}} \cdot \sqrt{\frac{\Phi(\sqrt{s})}{\Phi(M)}}, \quad (3)$$

where M, Γ_{tot}, Γ_{ee}, and $\mathcal{B}$ are the mass, full width, electronic partial width (whose definition includes vacuum polarization effects, that is why the dressed cross sections are fitted to rather than the Born cross sections), and branching fraction of corresponding resonance, respectively. $\Phi(\sqrt{s}) = \int\int \frac{1}{(2\pi)^3 32(\sqrt{s})^3} dm_{12}^2 dm_{23}^2$ is the three-body phase space [40], where m_{ij} is the invariant mass of particles i and j. The fitting curve is shown in Fig. 3, and the fit quality is estimated to be $\chi^2/\text{n.d.f} = 37.45/21$, where n.d.f is the number of degrees of freedom. The resonance with lower mass is consistent with the previously established $Y(4230)$. Its mass and width are determined to be $M(Y(4230)) = (4225.3 \pm 2.3)$ MeV and $\Gamma(Y(4230)) = (72.9 \pm 6.1)$ MeV. Since there is no observed state corresponding to the resonance with higher mass, we name it as $Y(4500)$. Its mass and width are determined to be $M(Y(4500)) = (4484.7 \pm 13.3)$ MeV, $\Gamma(Y(4500)) = (111.1 \pm 30.1)$ MeV, respectively. The statistical significance of $Y(4230)$ and $Y(4500)$ have been estimated to be 29σ and 8σ, respectively, via the differences of the likelihood values and the degrees of freedom with and without considering the corresponding resonance by the Wilk's theorem [47]. Two solutions with equal goodness-of-fit qualities are found. The masses and total widths are unchanged in the two solutions, while the amplitudes vary significantly due to constructive and destructive interferences between $Y(4230)$ and $Y(4500)$, which are consistent with the mathematical expectation of multiple solutions [48]. The products of the electron partial width and branching fraction, of the states $Y(4230)$ and $Y(4500)$, are listed in Table 1.

The main sources of systematic uncertainties of the cross section measurements are: the integrated luminosity $\mathcal{L}_{\text{int}}$, the tracking and PID efficiency, the branching fraction of $J/\psi \rightarrow \ell^+\ell^-$, kinematic fit, $(1+\delta)_{ISR}$, the intermediate structures of the K^+K^- system, the resolution of J/ψ, and the requirement on the penetration depth in the muon counter. The $\mathcal{L}_{\text{int}}$ is measured with Bhabha events and the uncertainty is found to be 1.0% [29, 30]. The dif-
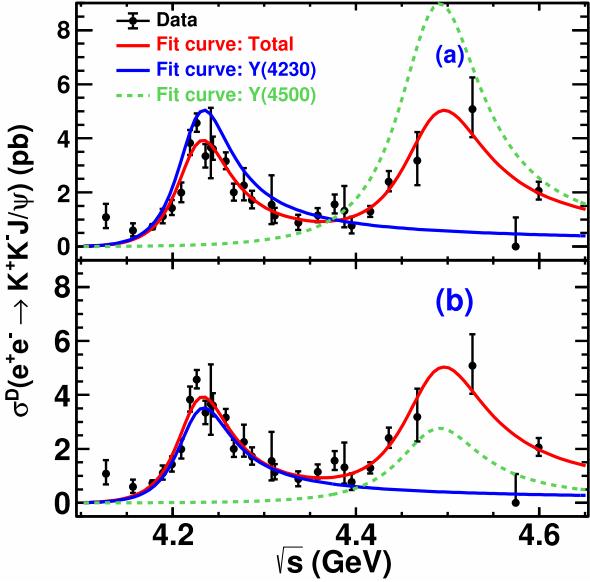
Fig. 3. (color online) Dressed cross sections of $e^+e^- \to K^+K^-J/\psi$, indicated by error bars with only statistical uncertainties. They are fitted by a coherent sum of two Breit-Wigner functions indicated by red solid curves, and the blue and pink dashed curves are the amplitudes describing the resonances $Y(4230)$ and $Y(4500)$, respectively. (a) corresponds to solution I, (b) corresponds to solution II.

Table 1. Fitted parameters of the two resonant structures observed in the cross sections of $e^+e^- \to K^+K^-J/\psi$, where the first uncertainty is statistical and the second one is systematic.

	Parameters	Solution I	Solution II
$Y(4230)$	M/MeV	$4225.3 \pm 2.3 \pm 21.5$	
	Γ_{tot}/MeV	$72.9 \pm 6.1 \pm 30.8$	
	$\Gamma_{ee}\mathcal{B}$/eV	$0.42 \pm 0.04 \pm 0.15$	$0.29 \pm 0.02 \pm 0.10$
$Y(4500)$	M/MeV	$4484.7 \pm 13.3 \pm 24.1$	
	Γ_{tot}/MeV	$111.1 \pm 30.1 \pm 15.2$	
	$\Gamma_{ee}\mathcal{B}$/eV	$1.35 \pm 0.14 \pm 0.07$	$0.41 \pm 0.08 \pm 0.13$
Phase angle	φ/rad	$1.72 \pm 0.09 \pm 0.52$	$5.49 \pm 0.35 \pm 0.58$

ferences between data and MC in the tracking and PID efficiencies are studied by using the process $e^+e^- \to K^+K^-\pi^+\pi^-$, and 2.5% per charged kaon is quoted [23]. For tracking efficiency of charged leptons, the systematic uncertainty is studied by using the process $\psi(3686) \to \pi^+\pi^-J/\psi(J/\psi \to \ell^+\ell^-)$, and 1.0% uncertainty per lepton is quoted [49]. The uncertainty of the branching fraction of $J/\psi \to \ell^+\ell^-$ is quoted as 0.4% [40]. The uncertainty of kinematic fit is estimated by correcting the corresponding track parameters, and the difference between the efficiencies with (default) and without this correction is quoted as the relevant uncertainty [50]. Varied line shape of the input cross sections is constructed by connecting each nearby points with a smooth curve. The

difference between the final cross sections with this new line shape and the nominal one is taken as the uncertainty of radiation correction. The uncertainty associated with the intermediate structures is estimated by weighting the PHSP MC samples according to the observed $M(K^+K^-)$ distribution of data, and the difference between the two efficiencies of the two methods is quoted as the corresponding uncertainty. To estimate the uncertainty according to the difference in the resolutions between data and MC samples, the efficiency is re-obtained by smearing the resolution of the J/ψ signal of the MC sample. The difference is quoted as the associated uncertainty. To consider the uncertainty of the criteria on the penetration depth in the muon counter, the difference between the final results with and without this criterion is adopted. The total uncertainties are calculated by summing all individual items in quadrature. They are energy dependent and vary from 8.6% to 11.1%. All the systematic uncertainties, including the individual and total, are listed in Appendix 4.

The systematic uncertainties for the parameters of resonances mainly come from c.m. energy measurements, the form and parameterization of the fit function, and the systematic uncertainties in the cross section measurements that will be discussed later. The c.m. energies were measured with $e^+e^- \to \mu^+\mu^-$ events and the uncertainties are determined correspondingly for different data samples [27, 28]. The associated systematic uncertainty is estimated by varying the c.m. energies during the fit. A three-body PHSP shape for a non-resonant component is added to the two coherent BW sum to estimate the uncertainty of the cross section description in the fit, which turns out to be negligible. The uncertainty of the formalism of the full width is estimated by replacing the Γ_{tot} with $\Gamma = \Gamma_{\text{tot}} \frac{\Phi(\sqrt{s})}{\Phi(M)}$ in the denominator of Eq. (3), where Γ_{tot} is the nominal width of the resonance. The systematic uncertainties due to cross section measurements can be divided into two categories. The first one is uncorrelated among the different c.m. energy points including kinematic fit, radiation correction, intermediate structures, and resolution of J/ψ. The associated uncertainty is estimated by considering them while doing the fit and comparing to the results obtained only considering statistical uncertainties of the cross sections. The second category of the systematic uncertainties is correlated and common for all data samples (5.1%), therefore only affects the $\Gamma_{ee}\mathcal{B}$. All of these uncertainties on the parameters of resonances are listed in Appendix 4.

IV. SUMMARY AND DISCUSSION

In summary, the Born cross sections of $e^+e^- \to K^+K^-J/\psi$ at c.m. energy from 4.127 to 4.600 GeV are measured with a new partial reconstruction method and larger data samples compared with Ref. [23]. Two reson-

ances are observed with high significance. One is consistent to the previous observed $Y(4230)$, and its mass and width are measured to be $M(Y(4230)) = (4225.3 \pm 2.3 \pm 21.5)$ MeV, $\Gamma(Y(4230)) = (72.9 \pm 6.1 \pm 30.8)$ MeV, where the first uncertainties are statistical and the second are systematic. The other one can not be assigned into any experimentally observed resonance, named as $Y(4500)$, and its mass and width are determined to be $M(Y(4500)) = (4484.7 \pm 13.3 \pm 24.1)$ MeV, $\Gamma(Y(4500)) = (111.1 \pm 30.1 \pm 15.2)$ MeV, respectively. There are also evidences of this new structure in the measurements of the cross sections of $e^+e^- \to \pi\pi J/\psi$ [7], even in the same channel K^+K^-J/ψ [21-23]. But only with additional data samples at BESIII and improved analysis method, this state has been observed with a significance more than 5σ for the first time. The mass of $Y(4500)$ is consistent with the prediction of the 5S-4D mixing scheme [24], the heavy-antiheavy hadronic molecules model [25] and the lattice quantum chromodynamics result for a $(c s \bar{c} \bar{s})$ state [26], while the width is 2σ larger than the prediction of Ref. [24]. More experimental measurements and theoretical studies are needed to reveal its nature.

For the first time, the state $Y(4230)$ has been observed in the $K\bar{K}J/\psi$ mode with the significance larger than 5σ. The product of the electronic partial width and the decay branching fraction is measured to be $\mathcal{B}(Y(4230) \to K^+K^-J/\psi)\Gamma(e^+e^- \to Y(4230)) = (0.29 \pm 0.02 \pm 0.10)$ eV or $(0.42 \pm 0.04 \pm 0.15)$ eV, according to different interferences, respectively. The ratio between the branching fractions of the $Y(4230)$ decaying into $K\bar{K}J/\psi$ and $\pi\pi J/\psi$ [7] are calculated and shown in Table 2. Author of Ref. [51] predicts the $K\bar{K}$ mode should be suppressed if the $Y(4230)$ is Λ_c baryonium. Even at present, no conclusion can be drawn due to the multiple solutions. However, once the physics solution is determined as done in Ref. [19], it will provide very useful information for understanding the nature of $Y(4230)$.

Table 2. The ratios between the branching fractions of the $Y(4230)$ decaying into $K\bar{K}J/\psi$ and $\pi\pi J/\psi$, depending on the various combinations of the multiple solutions.

	$K\bar{K}J/\psi$ Sol. I	$K\bar{K}J/\psi$ Sol. II
$\pi\pi J/\psi$ Sol. I	0.17 ± 0.02	0.25 ± 0.04
$\pi\pi J/\psi$ Sol. II	0.097 ± 0.017	0.14 ± 0.03
$\pi\pi J/\psi$ Sol. III	0.035 ± 0.004	0.051 ± 0.007
$\pi\pi J/\psi$ Sol. IV	0.020 ± 0.002	0.028 ± 0.004

V. ACKNOWLEDGEMENT

APPENDIX

1. Distributions of $M(\ell^+\ell^-)$ and $M(K^+K^-)$

Figure. A1 shows the distributions of the invariant mass of lepton pairs, $M(\ell^+\ell^-)$, for data and PHSP signal MC samples at various c.m. energies. Here, the J/ψ signal and sideband regions are indicated with red and blue arrows, respectively. In addition, the distributions of invariant mass of kaons, $M(K^+K^-)$, for data, PHSP signal MC, and weighted MC samples at various c.m. energies are shown in Fig. A2.

2. Born cross sections

The Born cross sections of $e^+e^- \to K^+K^-J/\psi$ and related quantities such as the c.m. energy, the integrated luminosity, the numbers of observed signal events, the efficiencies, the radiative correction factors, the vacuum polarization factors are listed in Table A1.

3. Definition of likelihood function

In the maximum likelihood fit to the dressed cross sections of $e^+e^- \to K^+K^-J/\psi$, the likelihood is constructed as:

$$L(\mu; \vartheta) = \prod_i^6 L_i(\mu_i; \vartheta_i) \prod_j^{22} L_j(\mu_j; \vartheta_j), \tag{A1}$$

where μ_i and μ_j are the numbers of observed signal events, ϑ_i and ϑ_j are the parameters in the likelihood functions, and L_i and L_j are the likelihood functions for the data samples with $\mu \le 10$ and $\mu > 10$, respectively.

The likelihood functions are defined variously according to the different numbers of observed events. For the data samples with $\mu \le 10$, the likelihood function is described by a Poisson function:

$$L_i(\mu_i; \vartheta_i) = P_i(\mu_i; \vartheta_i) = \frac{1}{\mu_i!} \vartheta_i^{\mu_i} e^{-\vartheta_i}, \tag{A2}$$

While for the data samples with $\mu > 10$, the likelihood function is described by an asymmetric Gaussian function:

$$
\begin{aligned}
L_j(\mu_j, \sigma_{1j}, \sigma_{2j}; \vartheta_j) &= G(\mu_j, \sigma_{1j}, \sigma_{2j}; \vartheta_j) \\
&= \begin{cases} \dfrac{1}{\sqrt{2\pi}\,(\sigma_{1j} + \sigma_{2j})} \, e^{-\frac{(\vartheta_j - \mu_j)^2}{2\sigma_{1j}^2}} &, \vartheta_j > \mu_j; \\[2em] \dfrac{1}{\sqrt{2\pi}\,(\sigma_{1j} + \sigma_{2j})} \, e^{-\frac{(\vartheta_j - \mu_j)^2}{2\sigma_{2j}^2}} &, \vartheta_j \le \mu_j; \end{cases}
\end{aligned}
\tag{A3}
$$
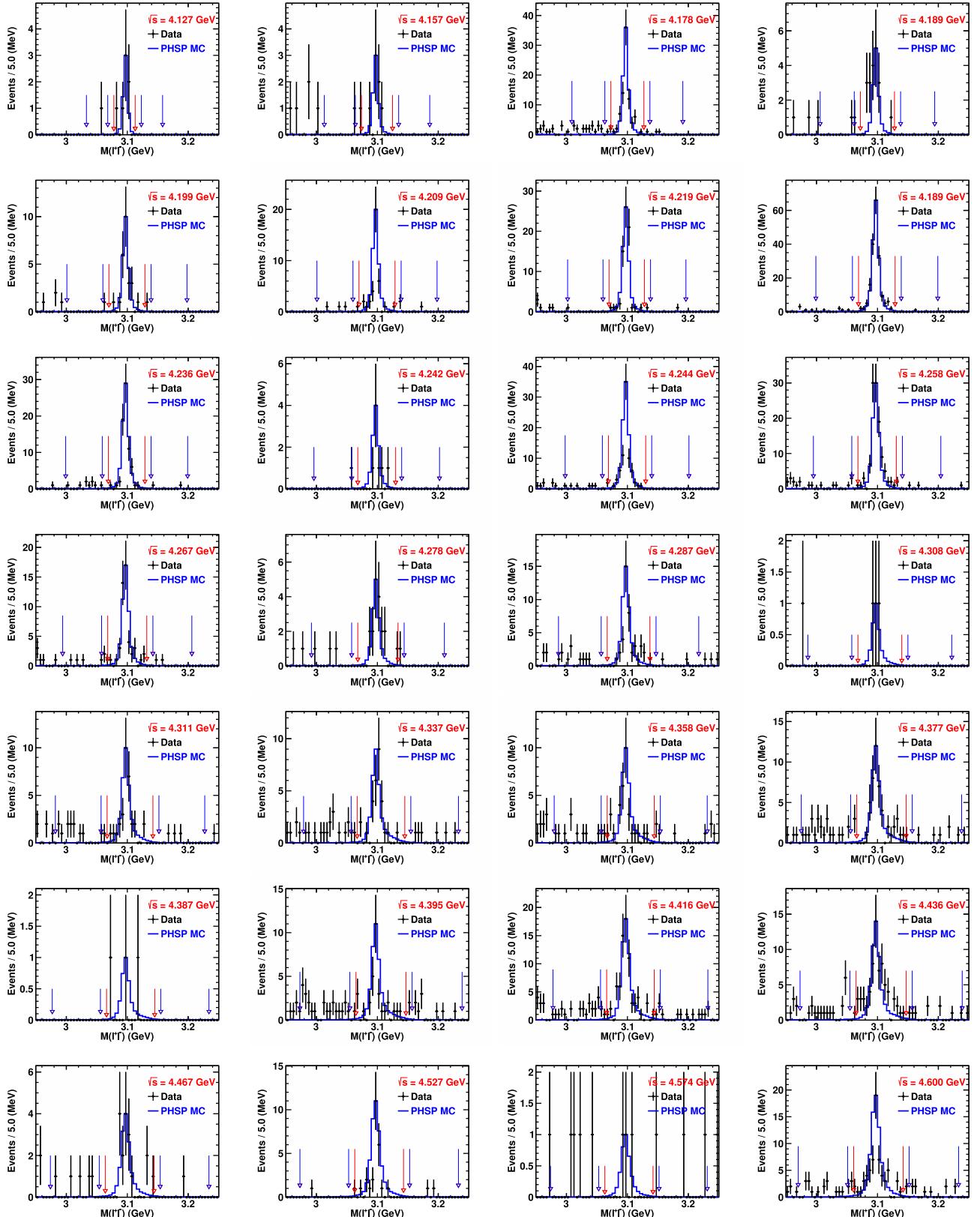
Fig. A1.   (color online) The distributions of invariant mass of lepton pairs $M(\ell^+\ell^-)$, where the dots with error bars are data, the blue histogram is PHSP signal MC sample (normalized to data), the red and blue arrows identify the J/ψ signal and sideband regions, respectively.
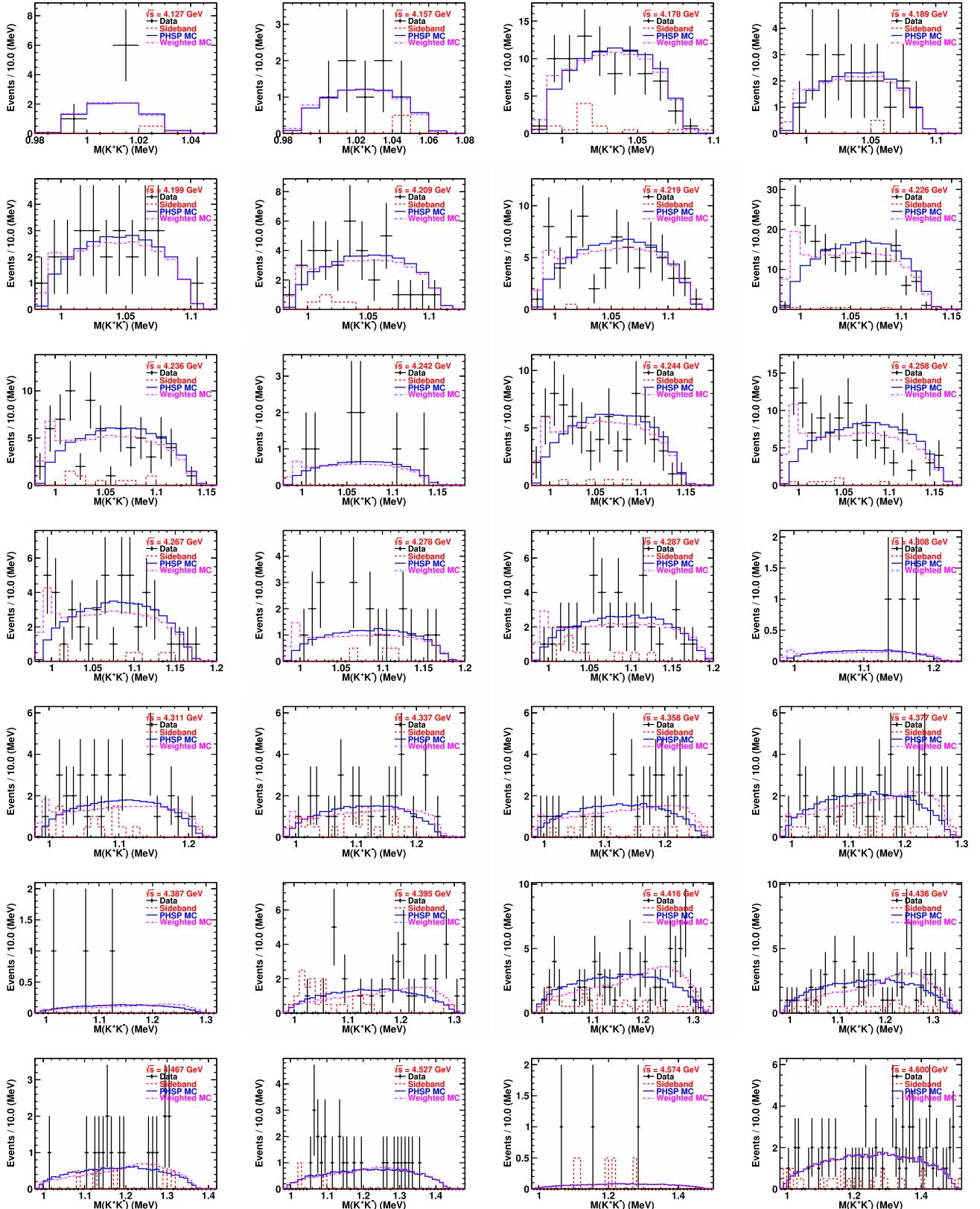
Fig. A2. (color online) The distributions of K^+K^- invariant mass of the data, PHSP signal MC and weighted MC samples at each c.m. energy, where the black dots with error bars indicate data from the J/ψ signal region, the red dashed curves indicate data from J/ψ sideband regions, the blue histograms indicate PHSP signal MC sample (normalized to data) and the yank dashed-dot curves indicate the weighted signal MC sample (normalized to data).

Table A1. The Born cross sections of $e^+e^- \to K^+K^-J/\psi$ and related quantities. Here $\sqrt{s}$ is the c.m. energy, $\mathcal{L}_{\mathrm{int}}$ is the integrated luminosity, N^{obs} is the number of observed signal events, ε is the efficiency, $(1+\delta)_{\mathrm{ISR}}$ is the radiative correction factor, $\frac{1}{|1-\Pi|^2}$ is the vacuum polarization factor, and the σ^{B} is the Born cross section, the first uncertainties are statistical, and the second systematic.

Data sample	$\sqrt{s}$/GeV	$\mathcal{L}_{\mathrm{int}}$/pb^{-1}	N^{obs}	ε	$(1+\delta)_{\mathrm{ISR}}$	$\frac{1}{\|1-\Pi\|^2}$	σ^{B}/pb
4130	4.127	401.50	$6.5^{+3.0}_{-2.4}$	0.141	0.896	1.052	$1.02^{+0.47}_{-0.38} \pm 0.09$
4160	4.157	408.70	$6.5^{+3.0}_{-2.4}$	0.263	0.856	1.053	$0.56^{+0.26}_{-0.21} \pm 0.05$
4180	4.178	3194.50	$72.0^{+9.7}_{-9.1}$	0.315	0.820	1.054	$0.69^{+0.09}_{-0.09} \pm 0.06$
4190	4.189	570.10	$18.5^{+4.7}_{-4.1}$	0.335	0.792	1.056	$0.97^{+0.25}_{-0.22} \pm 0.08$
4200	4.199	526.00	$25.0^{+5.2}_{-4.6}$	0.357	0.787	1.056	$1.34^{+0.28}_{-0.25} \pm 0.12$
4210	4.209	572.10	$33.5^{+6.4}_{-5.8}$	0.358	0.762	1.057	$1.70^{+0.33}_{-0.29} \pm 0.15$
4220	4.219	569.20	$69.0^{+8.7}_{-8.1}$	0.379	0.771	1.056	$3.29^{+0.41}_{-0.39} \pm 0.37$
4230	4.226	1100.90	$183.0^{+14.0}_{-13.3}$	0.395	0.771	1.056	$4.33^{+0.33}_{-0.31} \pm 0.38$
4237	4.236	530.30	$65.5^{+8.9}_{-8.3}$	0.391	0.789	1.056	$3.18^{+0.43}_{-0.40} \pm 0.30$
4245	4.242	55.88	$8.0^{+3.2}_{-2.5}$	0.405	0.805	1.055	$3.49^{+1.39}_{-1.09} \pm 0.31$
4246	4.244	538.10	$74.5^{+9.2}_{-8.5}$	0.393	0.812	1.056	$3.44^{+0.43}_{-0.39} \pm 0.30$
4260	4.258	828.40	$107.5^{+10.9}_{-10.3}$	0.396	0.866	1.054	$3.01^{+0.31}_{-0.29} \pm 0.26$
4270	4.267	531.10	$45.0^{+7.4}_{-6.7}$	0.390	0.911	1.053	$1.90^{+0.31}_{-0.28} \pm 0.17$
4280	4.278	175.70	$16.5^{+4.7}_{-4.0}$	0.372	0.935	1.053	$2.15^{+0.61}_{-0.52} \pm 0.19$
4290	4.287	502.40	$35.0^{+6.9}_{-6.3}$	0.363	0.937	1.053	$1.63^{+0.32}_{-0.29} \pm 0.14$
4310	4.308	45.08	$3.0^{+2.1}_{-1.4}$	0.367	0.982	1.052	$1.47^{+1.03}_{-0.69} \pm 0.13$
4315	4.311	501.20	$24.0^{+6.2}_{-5.6}$	0.358	0.985	1.052	$1.08^{+0.28}_{-0.25} \pm 0.10$
4340	4.337	505.00	$18.5^{+6.1}_{-5.6}$	0.364	0.963	1.051	$0.83^{+0.28}_{-0.25} \pm 0.07$
4360	4.358	544.00	$26.5^{+6.3}_{-5.7}$	0.378	0.935	1.051	$1.10^{+0.26}_{-0.24} \pm 0.10$
4380	4.377	522.70	$33.0^{+7.6}_{-7.1}$	0.379	0.891	1.051	$1.49^{+0.34}_{-0.32} \pm 0.13$
4390	4.387	55.57	$3.0^{+2.1}_{-1.4}$	0.397	0.865	1.051	$1.25^{+0.88}_{-0.58} \pm 0.11$
4400	4.395	507.80	$16.0^{+6.6}_{-6.1}$	0.401	0.861	1.051	$0.73^{+0.30}_{-0.28} \pm 0.06$
4420	4.416	1090.70	$57.0^{+9.4}_{-8.8}$	0.417	0.815	1.052	$1.23^{+0.20}_{-0.19} \pm 0.11$
4440	4.436	569.90	$55.5^{+8.9}_{-8.3}$	0.436	0.780	1.054	$2.28^{+0.37}_{-0.34} \pm 0.20$
4470	4.467	111.09	$14.0^{+4.6}_{-4.0}$	0.450	0.738	1.055	$3.02^{+0.99}_{-0.86} \pm 0.26$
4530	4.527	112.12	$23.5^{+5.4}_{-4.8}$	0.460	0.751	1.054	$4.82^{+1.11}_{-0.99} \pm 0.41$
4575	4.574	48.93	$0.0^{+2.3}_{-0.0}$	0.430	0.856	1.054	$0.00^{+1.01}_{-0.00} \pm 0.00$
4600	4.600	586.90	$52.0^{+8.7}_{-8.2}$	0.400	0.899	1.055	$1.96^{+0.33}_{-0.31} \pm 0.17$

where σ_1 and σ_2 are the upper and lower statistical uncertainties of μ, respectively.

4. The systematic uncertainties of the Born cross sections and the resonance parameters

The systematic uncertainties of the Born cross sections are listed in Table A2 and the systematic uncertainties of the resonance parameters are listed in Table A3. Figure. A3 shows dressed cross sections fitting results

with different function forms. Generally, there should be four solutions when three coherent amplitudes are used to describe a lineshape of cross sections. However, only two have been found by us. We suppose that the other solutions are very close to the found ones, then cannot be separated by the scanning method. And one should notice that the fitting results, with the tentatively additional continuum term, only change slightly.

Table A2. The systematic uncertainties (in units %) in the measurement of Born cross sections. Here $\sqrt{s}$ is the c.m. energy of data samples, $\mathcal{L}_{int}$ is the integrated luminosity, $\mathcal{B}(J/\psi \to l^+l^-)$ is the branching fraction, $(1+\delta)_{ISR}$ is the radiation correction factor, $M(K^+K^-)$ is the intermediate structures in K^+K^- system, $R(J/\psi)$ is the resolution of J/ψ, MUC is the criteria applied on the penetration depth in the muon counter.

Data sample	$\sqrt{s}$/GeV	$\mathcal{L}_{int}$	Tracking and PID	$\mathcal{B}(J/\psi \to l^+l^-)$	kinematic fit	$(1+\delta)_{ISR}$	$M(K^+K^-)$	$R(J/\psi)$	MUC	Total
4130	4.127	1.0	4.5	0.4	0.4	1.2	6.9	0.3	2.1	8.7
4160	4.157	1.0	4.5	0.4	0.7	0.7	6.9	0.3	2.1	8.6
4180	4.178	1.0	4.5	0.4	0.9	2.6	6.9	0.2	2.1	9.0
4190	4.189	1.0	4.5	0.4	1.0	1.0	6.9	0.1	2.1	8.7
4200	4.199	1.0	4.5	0.4	1.1	0.6	6.9	0.3	2.1	8.7
4210	4.209	1.0	4.5	0.4	1.1	1.7	6.9	0.3	2.1	8.8
4220	4.219	1.0	4.5	0.4	1.1	6.9	6.9	0.2	2.1	11.1
4230	4.226	1.0	4.5	0.4	1.1	0.6	6.9	0.4	2.1	8.7
4237	4.236	1.0	4.5	0.4	1.2	3.5	6.9	0.4	2.1	9.3
4245	4.242	1.0	4.5	0.4	1.2	2.4	6.9	0.2	2.1	9.0
4246	4.244	1.0	4.5	0.4	1.2	1.5	6.9	0.2	2.1	8.8
4260	4.258	1.0	4.5	0.4	1.3	1.3	6.9	0.3	2.1	8.8
4270	4.267	1.0	4.5	0.4	1.3	2.7	6.9	0.3	2.1	9.1
4280	4.278	1.0	4.5	0.4	1.3	1.3	6.9	0.4	2.1	8.8
4290	4.287	1.0	4.5	0.4	1.2	1.2	6.9	0.3	2.1	8.7
4310	4.308	1.0	4.5	0.4	1.6	1.3	6.9	0.4	2.1	8.8
4315	4.312	1.0	4.5	0.4	1.6	0.7	6.9	0.4	2.1	8.8
4340	4.337	1.0	4.5	0.4	1.6	1.5	6.9	0.7	2.1	8.9
4360	4.358	1.0	4.5	0.4	1.4	0.5	6.9	0.5	2.1	8.7
4380	4.377	1.0	4.5	0.4	1.4	0.3	6.9	0.6	2.1	8.7
4390	4.387	1.0	4.5	0.4	1.2	1.0	6.9	0.5	2.1	8.7
4400	4.395	1.0	4.5	0.4	1.1	0.9	6.9	0.5	2.1	8.7
4420	4.416	1.0	4.5	0.4	0.9	1.0	6.9	0.7	2.1	8.7
4440	4.436	1.0	4.5	0.4	0.7	1.6	6.9	0.6	2.1	8.8
4470	4.467	1.0	4.5	0.4	0.4	0.2	6.9	0.4	2.1	8.6
4530	4.527	1.0	4.5	0.4	0.3	0.9	6.9	0.6	2.1	8.6
4575	4.574	1.0	4.5	0.4	0.2	0.0	6.9	0.4	2.1	8.6
4600	4.600	1.0	4.5	0.4	0.2	1.2	6.9	0.3	2.1	8.7

Table A3. The systematic uncertainty in the measurement of the resonance parameters for solution I (solution II), where Non-Resonant indicated a three-body PHSP shape is added in the default fit and considering the coherent between them, the cross section$_1$ is uncorrelated systematic uncertainties from the measurement of cross sections, while cross section$_2$ is correlated.

Sources	Parameters						
	$Y(4230)$			$Y(4500)$			phase angle
	M/MeV	Γ_{tot}/MeV	$\Gamma_{ee}\mathcal{B}$/eV	M/MeV	Γ_{tot}/MeV	$\Gamma_{ee}\mathcal{B}$/eV	φ/rad
c.m. Energy	0.7	0.1	–	1.8	1.4	–	0.00 (0.02)
Non-Resonant	–	–	–	–	–	–	0.13 (0.51)
Γ_{tot}	21.5	30.8	0.15 (0.10)	24.1	15.1	0.02 (0.13)	0.50 (0.28)
cross section$_1$	–	–	– (–)	0.1	0.1	– (–)	–
cross section$_2$	–	–	0.02 (0.01)	–	–	0.07 (0.02)	–
Total	21.5	30.8	0.15 (0.10)	24.1	15.2	0.07 (0.13)	0.52 (0.58)
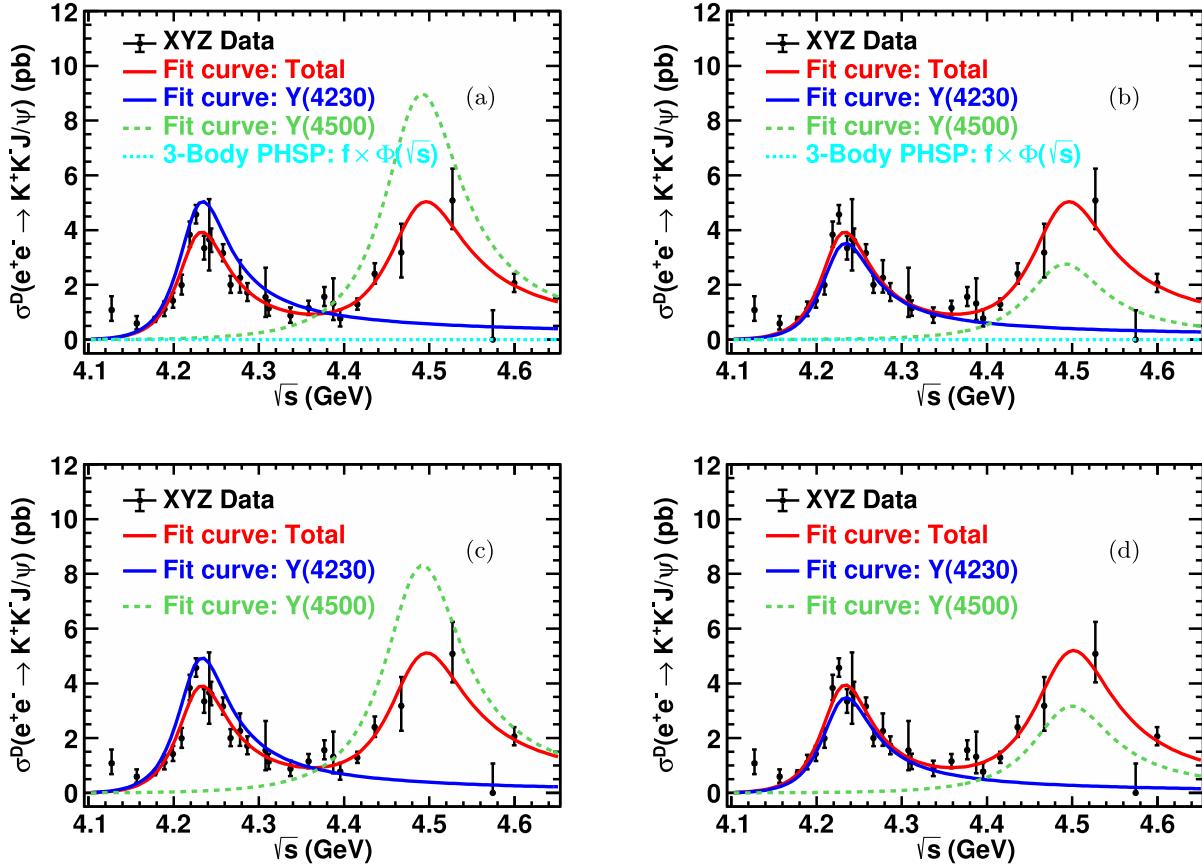
Fig. A3. (color online) The dressed cross sections fitting results with different function forms. (a), (b) are two sets of solutions to the sum of two coherent Breit-Wigner functions and 3-body phase space function fitting, respectively. (c), (d) are two sets of solutions to the two coherent Breit-Wigner functions with an energy-dependent full width fitting, respectively.

References

[1]   N. Brambilla *et al*., Phys. Rept **873**, 1 (2020)
[2]   B. Aubert *et al*. (BABAR Collaboration), Phys. Rev. Lett. **95**, 142001 (2005)
[3]   Q. He *et al*. (CLEO Collaboration), Phys. Rev. D **74**, 091104 (2006)
[4]   C. Z. Yuan *et al*. (Belle Collaboration), Phys. Rev. Lett. **99**, 182004 (2007)
[5]   M. Ablikim *et al*. (BESIII Collaboration), Phys. Rev. Lett. **118**, 092001 (2017)
[6]   M. Ablikim *et al*. (BESIII Collaboration), Phys. Rev. D **102**, 012009 (2020)
[7]   M. Ablikim *et al*. (BESIII Collaboration), (2022), arXiv: 2206.08554[hep-ex].
[8]   M. Ablikim *et al*. (BESIII Collaboration), Phys. Rev. Lett. **118**, 092002 (2017)
[9]   M. Ablikim *et al*. (BESIII Collaboration), Phys. Rev. D **96**, 032004 (2017)
[10] M. Ablikim *et al*. (BESIII Collaboration), Phys. Rev. D **97**, 052001 (2018)
[11] M. Ablikim *et al*. (BESIII Collaboration), Phys. Rev. D **104**, 052012 (2021)
[12] M. Ablikim *et al*. (BESIII Collaboration), Phys. Rev. Lett. **114**, 092003 (2015)
[13] M. Ablikim *et al*. (BESIII Collaboration), Phys. Rev. D **99**, 091103 (2019)
[14] M. Ablikim *et al*. (BESIII Collaboration), Phys. Rev. Lett. **122**, 102002 (2019)
[15] M. Ablikim *et al*. (BESIII Collaboration), Phys. Rev. Lett. **122**, 232002 (2019)
[16] K. Zhu, Inter. Jour. Mod. Phys. A **36**, 2150126 (2021)
[17] M. Ablikim *et al*. (BESIII Collaboration), Phys. Rev. D **102**, 031101 (2020)
[18] M. Ablikim *et al*. (BESIII Collaboration), Phys. Rev. D **101**, 012008 (2020)
[19] K. Zhu, Phys. Rev. D **105**, L031506 (2022)
[20] T. E. Coan *et al*. (CLEO Collaboration), Phys. Rev. Lett. **96**, 162003 (2006)
[21] C. Z. Yuan *et al*. (Belle Collaboration), Phys. Rev. D **77**, 011105 (2008)
[22] C. P. Shen *et al*. (Belle Collaboration), Phys. Rev. D **89**, 072015 (2014)
[23] M. Ablikim *et al*. (BESIII Collaboration), Phys. Rev. D **97**, 071101 (2018)
[24] J. Z. Wang, D. Y. Chen, X. Liu *et al*., Phys. Rev. D **99**, 114003 (2019)
[25] X. K. Dong, F. K. Guo, and B. S. Zou, Progr. Phys. **41**, 65

(2021), arXiv:2101.01021[hep-ph]

[26] T. W. Chiu and T. H. Hsieh (TWQCD Collaboration), Phys. Rev. D **73**, 094510 (2006)

[27] M. Ablikim *et al.* (BESIII Collaboration), Chin. Phys. C **40**, 063001 (2016)

[28] M. Ablikim *et al.* (BESIII Collaboration), Chin. Phys. C **45**, 103001 (2021)

[29] M. Ablikim *et al.* (BESIII Collaboration), Chin. Phys. C **39**, 093001 (2015)

[30] M. Ablikim *et al.* (BESIII Collaboration), (2022), arXiv: 2203.03133[hep-ex].

[31] M. Ablikim *et al.* (BESIII Collaboration), Chin. Phys. C **44**, 040001 (2020)

[32] M. Ablikim *et al.* (BESIII Collaboration), Nucl. Instrum. Meth. A **614**, 345 (2010)

[33] S. Agostinelli *et al.*, Nucl. Instrum. Meth. A **506**, 250 (2003)

[34] Z. Y. Deng *et al.*, Chin. Phys. C **30**, 371 (2006)

[35] S. Jadach, B. F. L. Ward, and Z. Was, Phys. Rev. D **63**, 113009 (2001)

[36] R. G. Ping, Chin. Phys. C **38**, 083001 (2014)

[37] R. G. Ping, Chin. Phys. C **32**, 599 (2008)

[38] D. J. Lange, Nucl. Instrum. Meth. A **462**, 152 (2001)

[39] P. Golonka and Z. Was, Eur. Phys. J. C, 97 (2006)

[40] P. Zyla *et al.* (Particle Data Group), PTEP **2020**, 083C01 (2020)

[41] J. C. Chen, G. S. Huang, X. R. Qi *et al.*, Phys. Rev. D **62**, 034003 (2000)

[42] R. L. Yang, R. G. Ping, and H. Chen, Chin. Phys. Lett. **31**, 061301 (2014)

[43] W. A. Rolke, A. M. López, and J. Conrad, Nucl. Instrum. Meth. A **551**, 493 (2005)

[44] I. Danilkin, D. A. S. Molnar, and M. Vanderhaeghen, Phys. Rev. D **102**, 016019 (2020)

[45] S. Actis *et al.* (Working Group on Radiative Corrections and Monte Carlo Generators for Low Energies), Eur. Phys. Jour. C **66**, 585 (2010)

[46] W. Y. Sun, T. Liu, M. Q. Jing *et al.*, Front. Phys. (Beijing) **16**, 64501 (2021)

[47] S. S. Wilks, Annals Math. Statist. **9**, 60 (1938)

[48] K. Zhu, X. H. Mo, C. Z. Yuan, and P. Wang, Int. J. Mod. Phys. A **26**, 4511 (2011)

[49] M. Ablikim *et al.* (BESIII Collaboration), Phys. Rev. D **91**, 112005 (2015)

[50] M. Ablikim *et al.* (BESIII Collaboration), Phys. Rev. D **87**, 012002 (2013)

[51] C. F. Qiao, Phys. Lett. B **639**, 263 (2006)